Supporting information

Coaxially-Enlarged Photocarrier Transport of Highly-oriented Cu_2ZnSnS_4/ZnO Photodetector Through the Nanoconfinement Effect

Wen Li,[a, ‡] Da Xiong,[a, ‡] Meilin Xie,[a] Chao Luo,[a] Xiankan Zeng,[a] Yue Gao,[a] Bolin Guo,[a] Cheng Yan,[a] Fengjun Chun,[a] Zhihao Zhu,[a] Xiaoqiang Fan,[a] Weili Deng,[a] Weiqing Yang*,[a]

[a] Key Laboratory of Advanced Technologies of Materials (Ministry of Education), School of Materials Science and Engineering, Southwest Jiaotong University, Chengdu 610031, China

‡ These authors contributed equally to this work.

*Corresponding Author E-mail: wqyang@swjtu.edu.cn

Tel.: +86-028-87601211; Fax: +86-028-87601211

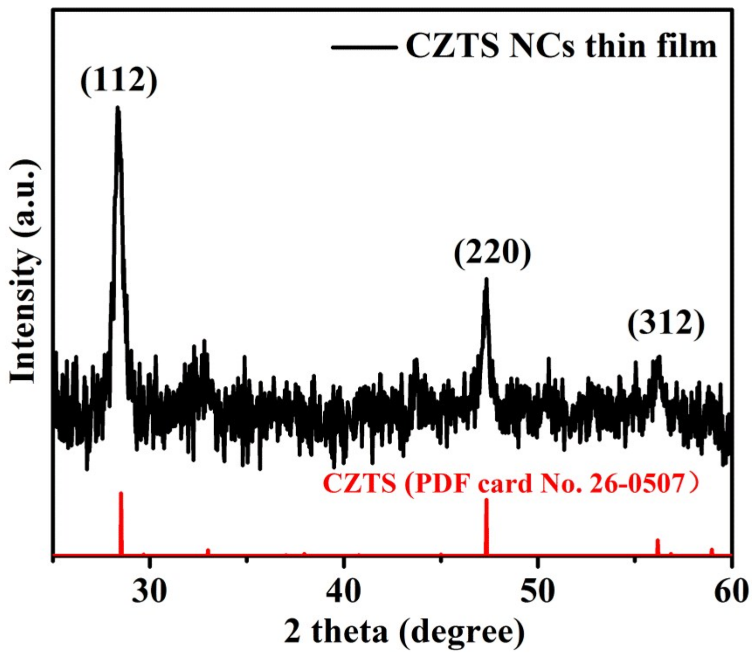

Figure S1 XRD of as-prepared CZTS nanocrystals.

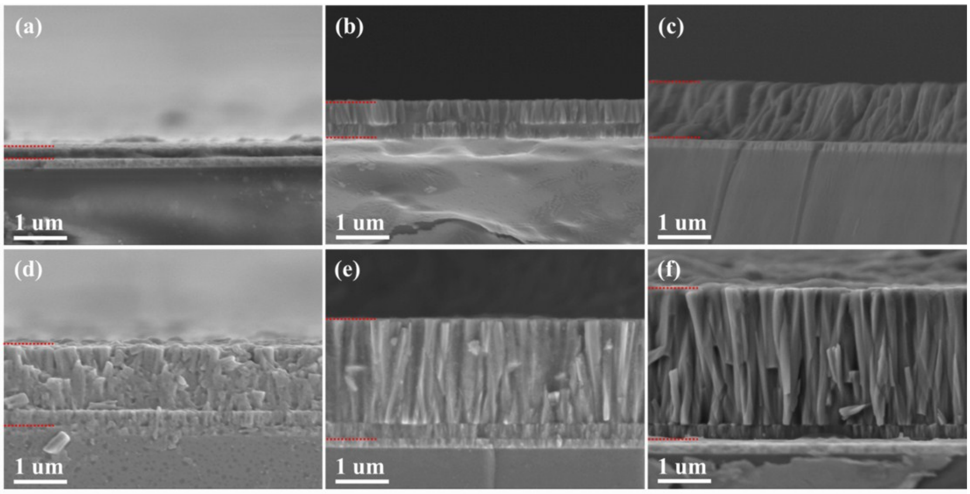

Figure S2 Cross-sectional SEM images of the ZnO nanorods array obtained with different growth time: (a) 1h, (b) 2h, (c) 3 h, (d) 4 h, (e) 5 h and (f) 6 h.

To investigate the effect of the ZnO NRs array on photocarriers transport of this device, highly-oriented ZnO NRs arrays with different lengths were prepared by changing the growth time. In Figure S2 (a–f), all images showed a floor layer about 0.3 μm on top of ITO substrate, this layer was ZnO seed layer. The length of the ZnO NRs was quantified from the cross-sectional SEM image. When the growth time increased from 1 h to 6 h, ZnO NRs were vertically well aligned on the ZnO seed layer, and its length reached to 2.8 μm. The ZnO films with 0.3 um and 2.3 um length were the poorly-oriented and highly-oriented ZnO films respectively.

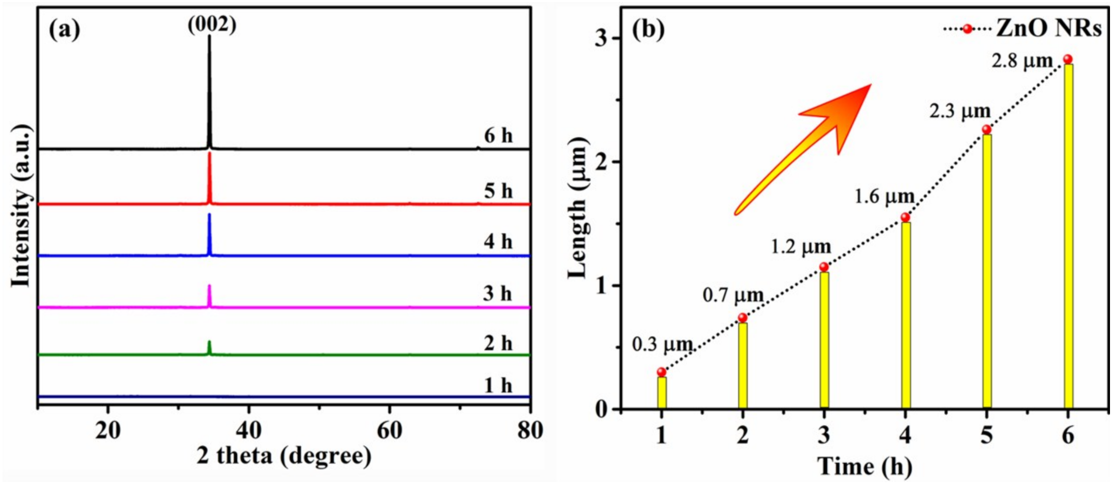

Figure S3 (a) XRD patterns of ZnO NRs array films, (b) the length of the ZnO NRs is plotted as a function of growth time.

Figure S3a displays XRD patterns of ZnO NRs array films, a characteristic peak with higher intensity at 34.4^{o} was observed, suggesting that the ZnO NRs preferentially oriented in the (002) direction parallel to *c*-axis. After increasing the growth time, the elevated intensity of (002) peak stated the improved crystallinity and extended length of ZnO NRs array. The length of the ZnO NRs is plotted as a function of growth time in Figure S3b. The average lengths of the highly c-axis-oriented ZnO arrays were almost linearly increased from 0.3 to 2.8 μm by prolonging the growth time.

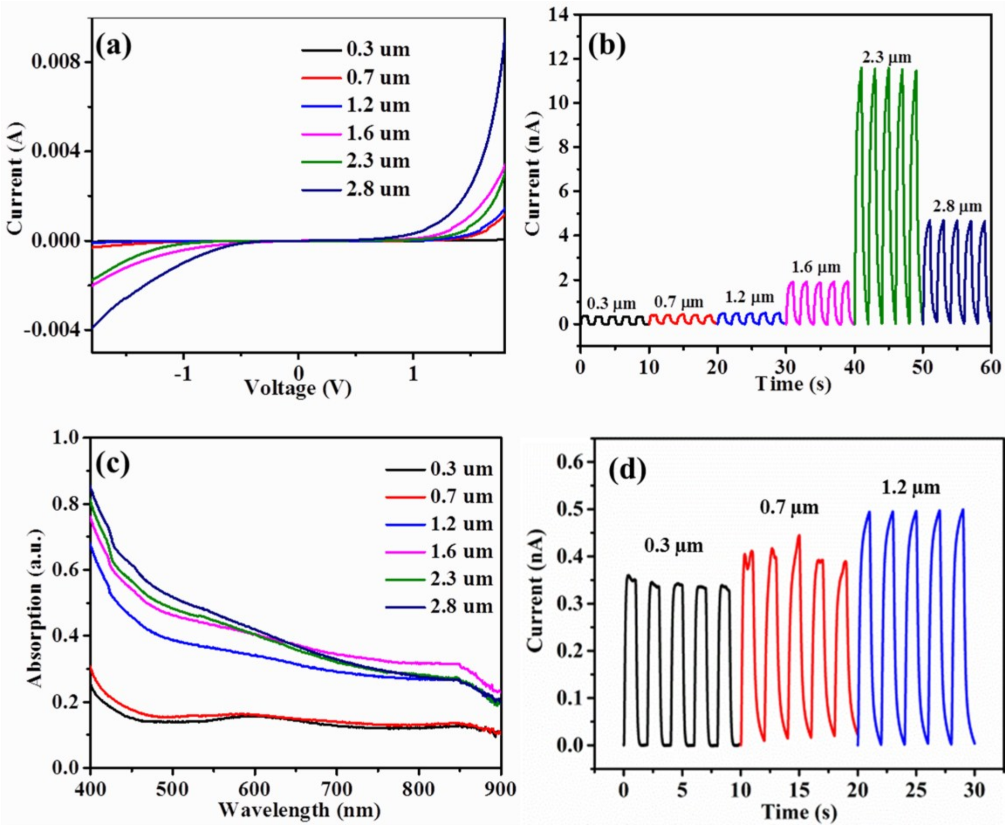

Figure S4 (a) I−V characteristic of photodetectors under dark conditions, (b) photoresponse behaviors under 450 nm (1.77 mW/mm^2) illumination without bias voltage, (c) absorption spectra, (d) a partial enlargement of Figure S4b.

Figure S4 showed the effects of ZnO NRs length on the device properties. These six photodetectors exhibit obvious rectifying curves (Figure S4a). However, when the preference orientation is less obvious equaling to the short lengths of ZnO films (0.3, 0.7 and 1.2 µm), the photocurrents were so low and only changes slightly (Figure S4d). Although there are continued significant increases in photocurrent after the preference growth direction is more perfect as the length of ZnO NRs array increased to 1.6 and 2.3 µm, while as the length is increased to 2.8 µm, the photocurrent of this device suddenly declined dramatically (Figure S4b). This trend is consistent with the description of mechanism shown in Figure 3d. The corresponding absorption spectra of these sample reveal that the absorption coefficient increases with the more highly *c*-axis-oriented ZnO NRs array (Figure S4c).

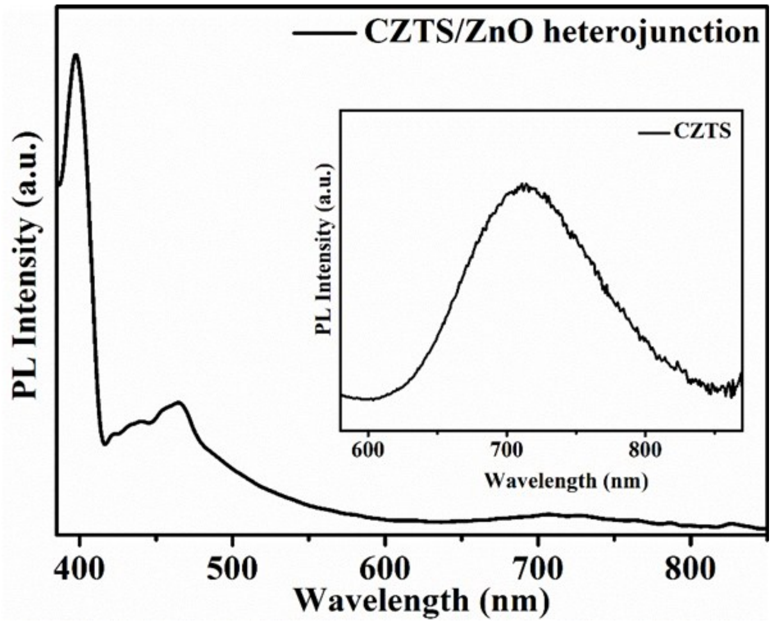

Figure S5 PL spectrum of the CZTS/ZnO heterojunction, the inset is the PL spectrum of CZTS film.

To understand the response mechanism of the photodetector, the room-temperature photoluminescence (PL) spectra acquired under 325 nm for the CZTS/ZnO heterojunction are investigated.